ACS OMEGA

Article

http://pubs.acs.org/journal/acsodf

Shortened Penetratin Cell-Penetrating Peptide Is Insufficient for Cytosolic Delivery of a Grb7 Targeting Peptide

Gabrielle M. Watson, Ketav Kulkarni, Rebecca Brandt, Mark P. Del Borgo, Marie-Isabel Aguilar, and Jacqueline A. Wilce*

Department of Biochemistry and Molecular Biology, Biomedicine Discovery Institute, Monash University, Wellington Road, Clayton, VIC 3800, Australia

ABSTRACT: Delivery across the cell membrane is of critical importance for the development of therapeutics targeting intracellular proteins. The use of cell-penetrating peptides (CPPs), such as Penetratin (P16), has facilitated the delivery of otherwise cell-impermeable molecules allowing them to carry out their biological function. A truncated form of Penetratin (RRMKWKK) has been previously described as the minimal Penetratin sequence that is required for translocation across the cell membrane. Here, we performed a detailed comparison of cellular uptake by Penetratin (P16) and the truncated Penetratin peptide (P7), including their ability to deliver G7-18NATE, a cyclic peptide targeting the cytosolic cancer target Grb7-adapter protein into cells. We identified that both P16 and P7 were internalized by cells to comparable levels; however, only P16 was effective in delivering G7-18NATE to produce a biological response. Live-cell imaging of fluorescein isothiocyanate-labeled peptides suggested that while P7 may be taken up into cells, it does not gain access to the cytosolic compartment. Thus, this study has identified that the P7 peptide is a poor CPP for the delivery of G7-18NATE and may also be insufficient for the intracellular delivery of other bioactive molecules.

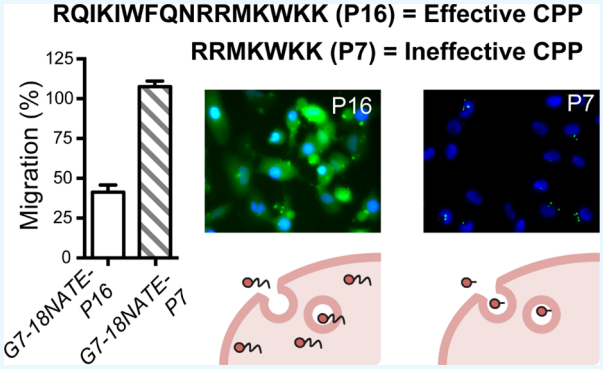

INTRODUCTION

Extensive progress has been made toward the development of biological agents targeted to intracellular protein−protein interfaces, as either tools for elucidating biochemical pathways or potential therapeutics.[1,2] Compared with small-molecule inhibitors, peptidic or oligonucleotide-based inhibitors show superior ability to selectively and potently bind to their targets. A shortcoming, however, is their general inability to diffuse across cellular membranes to reach their intracellular target. This was a major obstacle to the use of these molecules until the discovery of cell-penetrating peptides (CPPs).[3] CPPs are a group of short peptides, ranging from 8 to 30 amino acids that can readily translocate the cell membrane and deliver covalently or noncovalently bound functional biomolecules that would otherwise be cell-impermeable. Their entry into cells is facilitated by their predominantly hydrophobic character and, in some cases, their positive charge that allows for direct interactions with the lipid bilayer.[3] Their uptake mechanism is thought to involve a combination of direct permeation and endocytotic mechanisms depending on many factors, including the nature of the cargo, the cell type, the peptide concentration, the incubation time, and the CPP itself.[3,4] Cargos that have been efficiently delivered into the cytosol include proteins,[5,6] peptides,[7,8] and siRNA.[9,10] The efficient delivery of biologically active cargo by CPPs has thus opened up a major field of endeavor in biology as well as the possibility of developing biologic therapeutics against intracellular targets.

The first CPPs identified were found in naturally occurring proteins, including the HIV tat trans-activator protein and the *Drosphilia* Antennapedia homeodomain.[11−13] The 60-residue Antennapedia homeodomain was found to penetrate cells and induce strong morphological differentiation when added to a cell medium.[13] Subsequent studies narrowed down the sequence required for the translocation action to be residues 43−58 of the third α-helix of the homeodomain.[14] This 16-amino-acid sequence, RQIKIWFQNRRMKWKK, was named Penetratin (P16). In a follow-up study, a series of truncations was made to P16, leading to the identification of a shortened seven-residue peptide (residues 52−58; RRMKWKK, P7) as the minimal sequence that is required for cellular uptake.[15] The P7 peptide sequence was internalized, albeit with decreased efficiency compared to the full-length 16-residue sequence (~60%). Because of the ease of synthesis of a smaller peptide, this shortened CPP makes for an attractive peptide for the delivery of cargo for therapeutic applications.

In our laboratory, we have investigated an 11-residue cyclic peptide inhibitor, G7-18NATE, that targets the signaling

Received: January 3, 2017
Accepted: February 13, 2017
Published: February 23, 2017

DOI: 10.1021/acsomega.6b00561
ACS Omega 2017, 2, 670−677

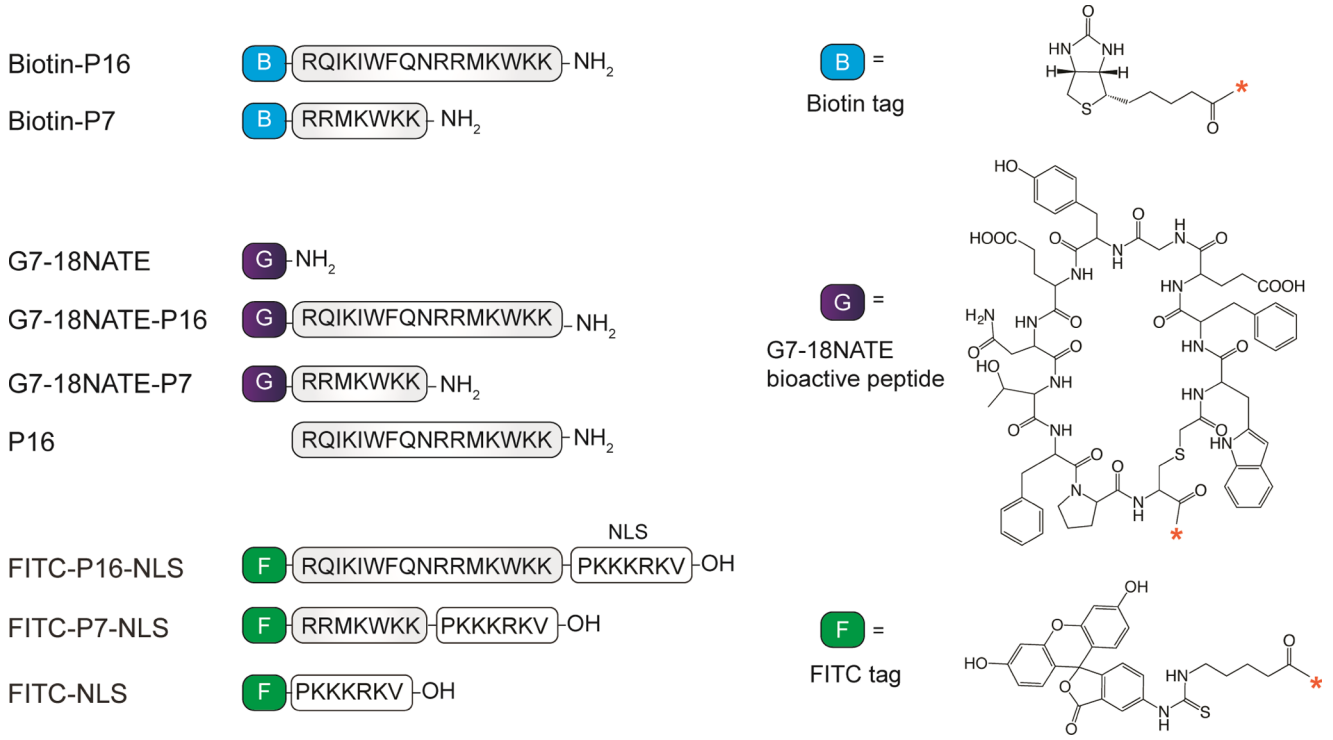

Figure 1. Schematic of peptides tested in this study. Sequences of P16 and P7 and the nuclear localization sequence (NLS) are shown in amino acid single-letter codes. Symbols B, F, and G represent the biotin, the fluorescein isothiocyanate (FITC), and the bioactive G7-18NATE peptide cargoes, respectively. The cargo chemical structures are shown with the attachment point to the CPP indicated by an orange asterisk.

adaptor protein—growth factor receptor bound protein 7 (Grb7). This signaling adaptor protein is a promising intracellular therapeutic target due to its overexpression in a large number of cancers, including breast, pancreatic, ovarian, esophageal, and gastric cancers.[16−20] Grb7 propagates signals from phosphorylated tyrosine kinases, such as HER2, HER3, and FAK, to promote migration, invasion, proliferation, and growth.[17,21−24] Grb7 binds to these upstream signaling partners via its C-terminal SH2 domain. Thus, it is this domain that the nonphosphorylated cyclic peptide G7-18NATE is targeted to, inhibiting the interactions of Grb7 with HER2, HER3, and FAK.[17,25]

To deliver G7-18NATE across the plasma membrane, G7-18NATE has been covalently linked to either of two CPPs, Tat or P16.[17,26] The CPPs were both effective in delivering G7-18NATE to the cytosol to inhibit Grb7 and effect a biological response. In HER2+ breast cancer cells, both G7-18NATE-P16 and G7-18NATE-Tat inhibited cell proliferation with EC_{50} values of approximately 8 and 50 μM, respectively, and G7-18NATE-P16 also displayed synergistic antiproliferative effects with the HER2 targeting molecules, doxorubicin and trastuzumab (herceptin).[27] In pancreatic and triple-negative breast cancer (TNBC) cells that overexpress Grb7, migration was shown to be significantly reduced following treatment with 10 μM G7-18NATE-P16, and in a pancreatic cancer mouse xenograft model, tumor growth and metastasis were significantly inhibited by G7-18NATE-P16 treatment.[17,26]

In an effort to create the minimal bioactive construct, we hypothesized that G7-18NATE could be conjugated to P7 for successful delivery to its Grb7 target in cells. In an earlier work using confocal microscopy imaging of fluorescent streptavidin, it appeared that such a biotin-labeled G7-18NATE-P7 construct efficiently co-localized with Grb7 in the cytosol.[28] Whether or not P7 could effectively deliver G7-18NATE to exert its biological activity was not investigated, which thus forms the basis of the study presented here.

Hence, we have investigated the effectiveness of the P7 peptide as a CPP for the cellular delivery of the G7-18NATE cargo in comparison to P16. Consistent with the original report, we have identified that biotinylated versions of the P16 and P7 peptides are internalized by cells to a similar extent. However, despite this apparent cellular internalization, only P16 was able to successfully deliver the G7-18NATE cargo to its target and achieve a biological response. We determined that this was unlikely to be due to the negative effects of the P7 peptide on Grb7-SH2 domain binding. Instead, we discovered that while P16 could effectively reach both the cytosol and nucleus of live TNBC cells, the P7 peptide did not permeate throughout these intracellular compartments and was potentially trapped in endosomes. Hence, we have identified that the truncated Penetratin sequence is insufficient to mediate the delivery of the G7-18NATE peptide to its intracellular cytosolic target. This study has important implications for the use of the shortened Penetratin delivery sequence as a delivery vehicle, for not only G7-18NATE but also all bioactive molecules that are being developed to target intracellular proteins.

RESULTS

P16 and P7 Delivery Sequences Appear To Be Internalized at Comparable Levels. It has been previously reported that the C-terminal seven residues of Penetratin (P7) constitute the minimal sequence required for internalization through the plasma membrane.[15] To investigate this further, we utilized the same experimental assay as originally used to identify this peptide: a peptide internalization assay that detects the presence of biotinylated peptide via treatment of cell lysate

DOI: 10.1021/acsomega.6b00561
ACS Omega 2017, 2, 670−677

with streptavidin-linked alkaline phosphatase, which is then quantified by the color produced by the enzymatic degradation of *p*-nitrophenol phosphate to *p*-nitrophenol. Both the full-length Penetratin (P16) and the C-terminal seven residues of Penetratin (P7) were synthesized with an N-terminal biotin group (see Figure 1 for a complete list of peptides utilized in this study).

We determined that, similar to previous findings, there was no significant difference in the level of intracellular biotin when HeLa cells were incubated with either Biotin-P16 or Biotin-P7, as determined by the absorbance at 405 nm (Figure 2). Because

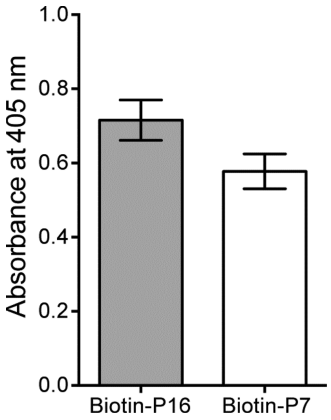

Figure 2. Cell internalization of biotin-labeled P16 and P7. HeLa cells were treated with either Biotin-P16 or Biotin-P7 (at 1 μM) for 15 min. The amount of internalized peptide was quantified by absorbance at 405 nm, as described in the Methods section. Error bars indicate the standard error of the mean (n = 3).

of the correlation between absorbance and internalized peptide, this assay suggested that both the Biotin-P16 and the Biotin-P7 were able to traverse the cell membrane with similar efficiency.

P7 Is Unable to Deliver the G7-18NATE Peptide Cargo. We next sought to determine whether the delivery sequences were equivalent in their ability to deliver a cargo to the cytosol. We thus prepared constructs, G7-18NATE-P16 and G7-18NATE-P7, in which P16 or P7 were synthesized C-terminal to G7-18NATE, the Grb7 targeting inhibitor (Figure 1). We conducted wound-healing migration assays using a TNBC cell line (MDA-MB-231) and a nonmalignant breast epithelial cell line (MCF-10A) to compare the ability of the peptides to decelerate cell migration, as shown previously for G7-18NATE-P16.[26] The level of inhibition was determined by comparing the cell-free area (at 12 h) between untreated and peptide-treated cells.

Consistent with previous reports, G7-18NATE-P16 lowered the rate of migration of the MDA-MB-231 cells by 41% compared to that of the untreated cells, whereas the P16 control did not decrease the rate of migration (Figure 3A,B). This demonstrated the ability of the P16 sequence to efficiently deliver the bioactive cargo to produce a functional inhibitory response in vivo. In contrast, when the G7-18NATE peptide was conjugated to the P7 sequence, the inhibitory effects of G7-18NATE were abolished (Figure 3A,B). The G7-18NATE-P7 construct had no effect on the rate of Grb7-induced cell migration.

Likewise, we found that G7-18NATE-P7 was unable to inhibit Grb7-mediated cell migration of MCF-10A cells (Figure 3A,C). In contrast, the effector peptide, G7-18NATE-P16, showed a 50% decrease in the migration rate compared to that of the untreated cells. Hence, in two separate cell lines, G7-18NATE-P16 but not G7-18NATE-P7 was effective at inhibiting migration.

P7 Does Not Negatively Interfere with Binding of G7-18NATE to Its Grb7-SH2 Target. To check that the lack of activity seen for G7-18NATE-P7 was not due to an inadvertent effect on its ability to bind to its intracellular target Grb7, we tested whether the two constructs could still bind to the Grb7-SH2 domain in vitro. For this, we used a Thermofluor-based thermal shift assay, which indicates ligand binding through the increased melting temperature of the target protein. The G7-18NATE peptides were incubated with both the Grb7-SH2 and the fluorophore Sypro Orange (which binds to the exposed hydrophobic regions). The temperature was increased incrementally, and the melting point of Grb7-SH2 was determined on the basis of the midpoint of the change in fluorescence intensity.

As displayed in Figure 4 and Table 1, G7-18NATE, G7-18NATE-P16, and G7-18NATE-P7 all bound to the Grb7-SH2 as indicated by an increased melting temperature of Grb7-SH2 (by 0.80, 0.74, and 1.80 °C, respectively). Representative unfolding curves are displayed in Figure 4, illustrating the way in which the unfolding curve is shifted upon addition of a 50 μM peptide. This is consistent with the binding of a biotin-labeled version of G7-18NATE-P7 previously shown by ITC to bind with an affinity of K_D = 14.4 μM.[28] Together, this shows that the attachment of either P16 or P7 does not negatively affect the binding of G7-18NATE to the Grb7-SH2 target.

P7 Does Not Reach the Cytosol. We thus speculated that the P7 peptide had the capacity to enter cells but not to deliver cargo fully into the cytosol of the cell. We therefore designed P16 and P7 constructs with an N-terminal FITC that would allow us to visualize the entry of the FITC-labeled peptides into live cells. To indicate cytosolic delivery, we also incorporated the NLS PKKKRKV so that only peptides that were successfully delivered into the cytosol would be able to be transported (by importin-α) into the nucleus of the cell.

The P16 and P7 peptides (with a FITC label at the N-terminus and an NLS sequence at the C-terminus) were synthesized and introduced to live MDA-MB-231 cells at 20 μM. As shown in Figure 5, after treating the cells for 20 min, FITC-P16-NLS was diffuse throughout the cytosol and nucleus, indicating that the peptide successfully reached the cytosol and was efficiently trafficked to the nucleus. In contrast, FITC-P7-NLS could only be seen sporadically in punctate structures in the cell. Furthermore, the fluorescence intensity was significantly diminished compared to that of the longer construct, suggesting limited retention of the internalized peptide or reduced fluorescence output due to a lower-pH environment. Both explanations would be consistent with an endosomal compartmentalization of the FITC-P7-NLS peptide. The fluorescently labeled NLS (FITC-NLS) control peptide was not observed in either the cytosol or the nucleus, confirming that this peptide was not internalized through the cell membrane to any observable extent. Thus, only the P16 sequence, and not the P7 sequence, was successfully delivered to the cytosol of the cell.

DISCUSSION

The development of therapeutics for intracellular targets is greatly hindered by the inability of the therapeutic molecule to pass through the plasma membrane. The conjugation of CPPs,

DOI: 10.1021/acsomega.6b00561
ACS Omega 2017, 2, 670−677

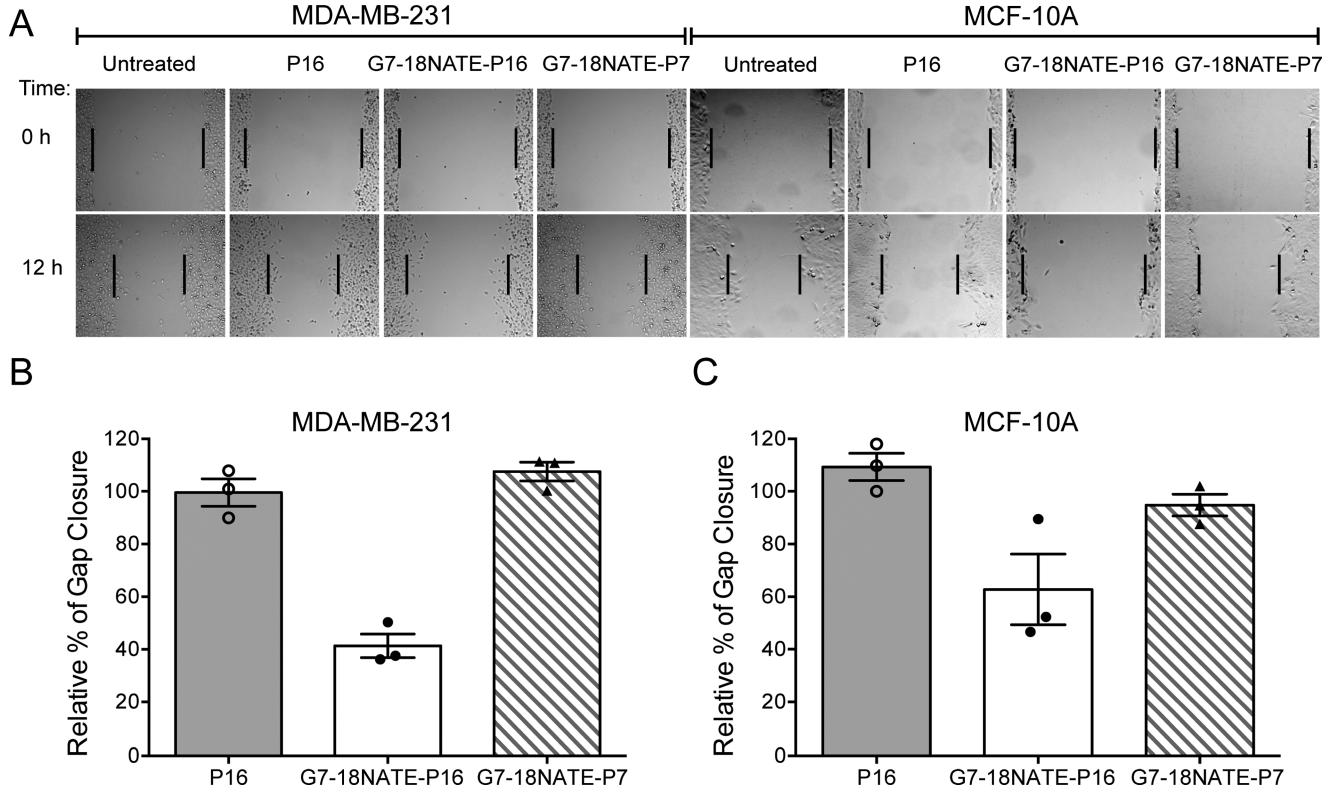

Figure 3. Wound-closure migration assay to determine the effect of Grb7 targeting peptides on cell migration. A cell-free gap was created in a confluent well of cells, and the movement of the cells was monitored in real-time, with images captured every 30 min for a 12 h period (cells maintained at 37 °C, 5% CO_2). The peptides (P16, G7-18NATE-P16, and G7-18NATE-P7) were added to the cell medium along with 1 ng.mL^{-1} epidermal growth factor (EGF). The remaining cell-free gap was measured using ImageJ and normalized, with 100% representing the movement of untreated cells. The error bars displayed indicate the standard error of the mean ($n \geq 3$), with each data point also displayed. (A) Representative cell images, (B) MDA-MB-231 cells, and (C) MCF-10A cells.

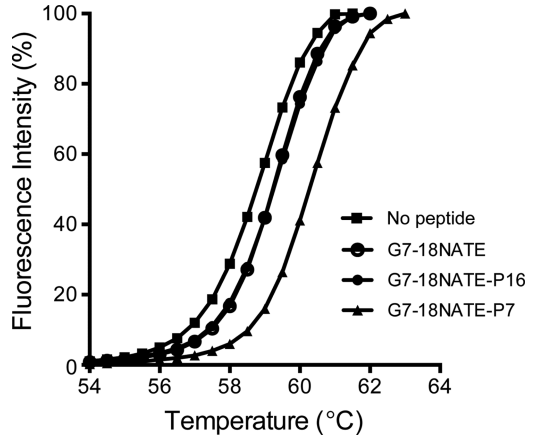

Figure 4. Thermofluor assay to determine the effect of peptides on the melting temperature of Grb7-SH2. The melting temperature of Grb7-SH2 was determined on the basis of the fluorescence intensity of the Thermofluor Sypro Orange in the absence or presence of peptide (G7-18NATE, G7-18NATE-P16, and G7-18NATE-P7). Representative unfolding curves with the fluorescent signal normalized to 100 and 0% on the basis of the experimentally determined maximum and minimum intensities, respectively.

such as Penetratin, to the bioactive molecule has dramatically improved the cellular uptake of otherwise impermeable molecules, such as peptides, proteins, and siRNA. When attached to Penetratin, the cyclic peptide, G7-18NATE, is a successful inhibitor of Grb7, an established anticancer target.[17]

Table 1. Effect of the Penetratin-Coupled G7-18NATE Peptides on the Melting Temperature of Grb7-SH2

peptide	change in T_m (°C)[a]
G7-18NATE	0.80 ± 0.26
G7-18NATE-P16	0.74 ± 0.09
G7-18NATE-P7	1.80 ± 0.14

[a]The reported error is the standard error of the mean (n = 3).

G7-18NATE has also previously been conjugated to the shortened Penetratin sequence, RRMKWKKK, and appeared to co-localize with Grb7 throughout the cytosol.[28] Therefore, to further investigate the potential of RRMKWKKK (P7) as a therapeutic delivery vehicle, we have functionally characterized P7 and G7-18NATE-P7 compared with their full-length Penetratin counterparts (P16 and G7-18NATE-P16).

We identified that biotinylated versions of both P16 and P7 CPPs were internalized to comparable levels into fixed HeLa cells. This was consistent with an earlier report, in which the same method was used to assess the uptake of a series of N- and C-terminal truncated Penetratin peptides into HaCaT cells (a human fibroblast cell line) and A549 cells (a human lung cancer cell line).[15] In this study, P7 was found to be the minimal sequence to efficiently cross membranes (~60% compared to that of the P16 sequence). This suggested that P7 should be an effective CPP for delivering G7-18NATE. However, we observed that when P16 or P7 was conjugated to G7-18NATE, only the G7-18NATE-P16 peptide was successful at producing the biological response of migration inhibition in

DOI: 10.1021/acsomega.6b00561
ACS Omega 2017, 2, 670−677

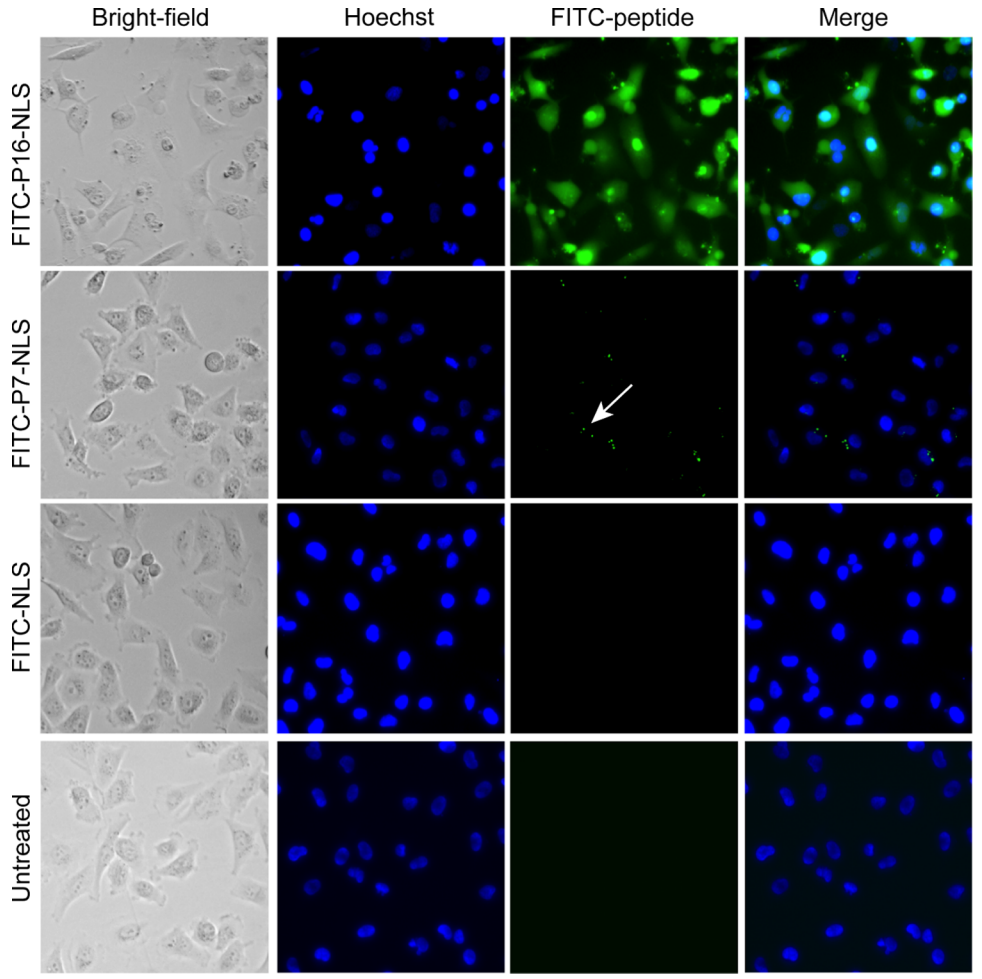

Figure 5. P16 peptide is efficiently internalized and localized to the cytosol and the nucleus. MDA-MB-231 cells were seeded (50 000) in 24-well plates and grown until ∼70% confluent. The growth media was replaced with the peptide-treated media (as indicated on the left panel) and incubated for 20 min at 37 °C, before being gently washed and imaged using a 20× objective lens (green indicates the presence of the FITC-labeled peptide). The white arrow indicates punctate structures corresponding to the FITC-labeled peptide. The Hoechst dye (blue channel) was incorporated to allow the detection of the nucleus.

the MDA-MB-231 and MCF-10A cells. This was surprising and suggested that the G7-18NATE-P7 construct was either not able to bind to its Grb7 target or not reaching the cytosolic compartment, where Grb7 exists. We showed, using a thermal shift assay, that G7-18NATE-P7 was still able to bind to the Grb7-SH2 domain; therefore, we next compared the abilities of P7 and P16 to not only enter cells but also reach the cytosol. For this experiment, an NLS sequence was included so that any observation of nuclear localization would indicate that the peptide had reached the cytosol, where nuclear localization factors reside. We demonstrated that FITC-P16-NLS was successful in reaching the cytosol when visualized in live cells, whereas FITC-P7-NLS did not display a uniform cytosolic distribution, with only faint punctate structures visible in the MDA-MB-231 cells. Together, this shows that P7 is insufficient for the delivery of the G7-18NATE peptide and suggests that this may be due to its inability to fully penetrate the cellular membrane to reach the cytosol.

The P7 peptide has been used in several studies because of its ability to traverse cell membranes.[15] In some cases, a successful delivery has been reported. A photoactivatable form of the P7 peptide (through the attachment of photocleavable groups on the lysines) showed uptake in various cancer cell lines when tested using flow cytometry.[29] Furthermore, in a study by the Yang group, the chemotherapeutic doxorubicin attached to the Penetratin-derived sequence, CKRRMKWKK, displayed improved cellular uptake and antiproliferative effects compared to those of the doxorubicin treatment alone.[30]

In contrast to these successful reports of internalization, the Nielsen group reported a negligible uptake of the sequence FQNRRMKWKK compared to that of the full-length Penetratin sequence.[31] Likewise, for insulin absorption, it was demonstrated that only the full-length Penetratin sequence, and not the shorter NRRMKWKK, could facilitate the delivery of insulin through nasal mucosa.[32] Brock and co-workers have reported that the truncated peptide, NRRMKWKK, showed a poor translocation efficiency when tested by fluorescence correlation microscopy on live cells. However, when conjugated to the tyrosine kinase peptide inhibitor, the truncated peptide showed a greatly enhanced cellular uptake.[33] Whether or not this uptake is correlated to bioactivity was not reported in this study.

The different conclusions made for the P7 peptide may, in part, result from the differences in the experimental methods used. A confounding factor that has led to discrepancies between the observed cellular uptake and the bioactivity of

DOI: 10.1021/acsomega.6b00561
ACS Omega 2017, 2, 670−677

CPPs and CPP-cargo constructs is that, once cells are fixed, there is no distinction between the peptides that have reached the cytosol and the peptides that have entered the cell via endocytosis but remained trapped in the endosomes. Lebleu and co-workers identified that fixation techniques can lead to misleading conclusions by redistributing the membrane-bound and vesicle-entrapped peptide into the cytosol and the nucleus following permeabilization of the membrane.[34] Indeed, the initial experiment that identified P7 as the minimal sequence required for internalization was also conducted on fixed cells.[15] This may also be the reason we observed the uptake of P7 into cells, yet with no bioactivity.[28] As our study using live cells showed, the FITC-P7 peptide only appeared in punctate structures in the cell, consistent with the endosomal entrapment.

The reason for the dramatic difference between the abilities of P16 and P7 to traverse cell membranes and deliver cargo likely relates to their relative abilities to interact with and penetrate lipid bilayers. In a recent study, conducted using dual-polarization interferometry (DPI), we investigated the interactions of P16 and a truncated Penetratin derivative (RRMKWKKK-Biotin) with model membranes.[35] This revealed that P16 has a greater ability to interact with fluid-phase POPC/POPG membranes than the truncated derivative. Furthermore, kinetic modeling of the DPI data suggested that only the full-length sequence was able to fully bind to the membrane and disrupt the bilayer, whereas the truncated Penetratin made transient interactions that had no effect on the bilayer structure. Thus, the P7 peptide, despite its overall similar composition to the full-length P16, may be unable to sufficiently interact with the lipid bilayer to enable entry to the cytosol of the cell.

In conclusion, this study has highlighted that the shortened Penetratin delivery sequence is ineffective as a CPP. For efficient internalization to the cytosol of live cells and for the delivery of bioactive molecules, the full-length Penetratin sequence is required.

METHODS

Cell Culture. All cell lines were obtained from the American Type Culture Collection (ATCC) and passaged using standard techniques. The HeLa cell line was maintained and tested in Dulbecco's modified Eagle medium (DMEM) high glucose, 10% fetal calf serum (FCS), and 1% antibiotic−antimycotic (ABAM) solution. The MDA-MB-231 cell line culture medium was Roswell Park Memorial Institute (RPMI) Medium 1640 (Gibco) supplemented with 9.5% FCS, 0.25 IU mL^{-1} human insulin (Actrapid Penfill), and 20 mM HEPES (Gibco). The MCF-10A culture medium consisted of DMEM/F12 (Gibco) supplemented with 5% horse serum, human insulin (10 μg mL^{-1}), hydrocortisone (0.5 μg mL^{-1}), EGF (20 ng mL^{-1}), and cholera toxin (100 ng mL^{-1}).

Peptide Synthesis. All peptides were prepared, either commercially (Purar Chemicals, Australia) or in-house, by solid-phase peptide synthesis using Fmoc chemistry and Rink amide resin (except for FITC-labeled peptides, which utilized Fmoc-Val-Wang resin) and cleavage from the resin using standard procedures. The solution concentration of the peptides was determined spectrophotometrically at 280 nm using extinction coefficients determined from the amino acid content,[36] except for FITC-labeled peptides that were quantitated on the basis of the absorbance of fluorescein at 498 nm.[37]

Biotinylated Penetratin Biotin-P16 (biotin-ahx-RQIKIWFQNRRMKWKK, where ahx = 1,6-aminohexanoic acid) was prepared with biotin linked N-terminally via the ahx group that served as a spacer. The peptide was purified to homogeneity using reversed phase high-performance liquid chromatography (RP-HPLC), and its identity was confirmed using mass spectrometry (calcd m/z $(C_{120}H_{194}N_{38}O_{22}S_2)^{5+}$: 517.7; found $(C_{120}H_{194}N_{38}O_{22}S_2)^{5+}$: 518.1).

Biotinylated N-terminal seven residues of Penetratin Biotin-P7 (biotin-βG-RRMKWKK, where βG = β-glycine) was prepared with biotin linked N-terminally via the β-glycine residue that served as a spacer. The peptide was purified to homogeneity using RP-HPLC, and its identity was confirmed using mass spectrometry (calcd m/z $(C_{59}H_{101}N_{21}O_{10}S_2)^{4+}$: 332.9; found $(C_{59}H_{101}N_{21}O_{10}S_2)^{4+}$: 333.0).

The control peptides Penetratin P16 (RQIKIWFQNRRMKWKK) and G7-18NATE (cyclo-CH2CO-WFEGYDNTFPC) were prepared as reported previously.[35,38]

Cargo-containing peptides G7-18NATE-P16 (cyclo-(CH2CO-WFEGYDNTFPC-RQIKIWFQNRRMKWKK)) and G7-18NATE-P7 (cyclo-(CH2CO-WFEGYDNTFPC-RRMKWKK)) were synthesized as a continuous peptide chain and then cyclized via the formation of thioether between the N-terminus and the cysteine side chain post cleavage, as described for G7-18NATE.[38] The peptides were purified to homogeneity using RP-HPLC, and their identities were confirmed using mass spectrometry; G7-18NATE-P16 (calcd m/z $(C_{171}H_{246}N_{48}O_{38}S_2)^{6+}$: 608.3; found $(C_{171}H_{246}N_{48}O_{38}S_2)^{6+}$: 608.6) and G7-18NATE-P7 (calcd m/z $(C_{113}H_{159}N_{31}O_{26}S_2)^{5+}$: 487.03; found $(C_{113}H_{159}N_{31}O_{26}S_2)^{5+}$: 487.25).

FITC-labeled peptides FITC-P16-NLS (FITC-ahx-RQIKIWFQNRRMKWKK-PKKKRKV), FITC-P7-NLS (FITC-ahx-RRMKWKK-PKKKRKV), and FITC-NLS (FITC-ahx-PKKKRKV) were prepared with FITC linked N-terminally via the ahx group (1,6-aminohexanoic acid), which served as a spacer. The peptides were purified to homogeneity using RP-HPLC, and their identities were confirmed using mass spectrometry; FITC-P16-NLS (calcd m/z $(C_{171}H_{266}N_{50}O_{33}S_2)^{6+}$: 603.0; found $(C_{171}H_{266}N_{50}O_{33}S_2)^{6+}$: 603.46), FITC-P7-NLS (calcd m/z $(C_{113}H_{179}N_{33}O_{21}S_2)^{4+}$: 600.59; found $(C_{113}H_{179}N_{33}O_{21}S_2)^{4+}$: 601.03), and FITC-NLS (calcd m/z $(C_{67}H_{100}N_{16}O_{14}S)^{3+}$: 462.58; found $(C_{67}H_{100}N_{16}O_{14}S)^{3+}$: 462.72).

Peptide Internalization Assay. HeLa cells were seeded in 96-well plates (30 000 cells per well) in a culture medium. After 24 h, the media was replaced with a media containing the peptide of interest (at 1 μM) and incubated for 15 min. The cells were washed three times in ice-cold phosphate-buffered saline (PBS), fixed with 4% paraformaldehyde and permeabilized with 0.5% Tween20/PBS. The endogenous alkaline phosphatase activity was neutralized by incubating the plates at 65 °C for 60 min. The cells were blocked using 3% bovine serum albumin (BSA)/PBS and treated with streptavidin APase (1 μg mL^{-1} in 0.1% BSA/PBS) for 30 min at room temperature. Following three times washing with PBS, 50 μL of 100 $mg.mL^{-1}$ p-nitrophenol phosphate was introduced and incubated for 30 min at room temperature. The enzyme reaction was quenched using 2 M NaOH. The absorbance was measured at 405 nm using FLUOstar Omega. The samples were measured in triplicates, and the background absorbance was determined using untreated cells and subtracted from the

DOI: 10.1021/acsomega.6b00561
ACS Omega 2017, 2, 670−677

test conditions. The statistical analysis was performed using GraphPad Prism6 (GraphPad Software, CA).

Wound-Closure Migration Assay. The MDA-MB-231 or MCF-10A cells were seeded until confluent in 24-well plates, wounded with a sterile pipette tip to create a cell-free gap and cell debris cleared away with fresh media. Lyophilized peptides were resuspended in sterile MQ, diluted to the appropriate concentration in fresh media, and added to the appropriate wells, with each treatment duplicated. The media also contained 1 ng mL^{-1} EGF to stimulate migration. The Leica AF6000 LX live-cell-imaging system was used to capture images in real time (at 37 °C, 5% CO_2), with images collected every 30 min from a minimum of five positions per well. The remaining gap area was measured using ImageJ (Fiji) at 0 and 12 h and averaged from all measured positions across the duplicates. At least three independent experiments were performed. To allow for a direct comparison, the results are displayed as the relative percentage of gap closure compared with the untreated control cells normalized to 100%.

Cellular Uptake Assay. MDA-MB-231 cells were seeded (50 000) in 24-well plates and grown until 60−70% confluent. The media was replaced with the peptide-treated media (at 20 μM) and incubated for 20 min at 37 °C. The cells were washed gently three times with the growth media and incubated with Hoechst-treated media (1 μM) for 5 min at 37 °C before being transferred to the Leica AF6000 LX live-cell-imaging system. Here, the cells were maintained at 37 °C and 5% CO_2, and images were taken within 15 min using a 20× objective lens.

Expression and Purification of the Grb7-SH2 Domain. Grb7-SH2 (415−532 residues) was incorporated into the pGex2T plasmid and expressed and purified, as described previously.[39]

Thermal Shift Assays. The lyophilized peptides of interest were resuspended in 50 mM $NaPO_4$, 150 mM NaCl, 1 mM dithiothreitol, and 5% (v/v) dimethyl sulfoxide (DMSO) and tested at a final concentration of 50 μM. Grb7-SH2, dialyzed in the same buffer (excluding DMSO), was tested at 40 μM. Using Rotor-Gene 3000 (Corbett Life Science), the temperature was increased in 0.5 °C increments from 50 to 70 °C with a holding time of 60 s. The wavelength of excitation/emission was measured at 530/555 nm. Each condition was measured in duplicate or triplicate with values averaged. Peptide-only and buffer-only control samples were measured and subtracted from the averaged test measurements. At least three independent experiments were conducted. The statistical analysis was performed using GraphPad Prism6 (GraphPad Software, CA).

AUTHOR INFORMATION

Corresponding Author

*E-mail: jackie.wilce@monash.edu. Phone: + 613 9902 9226. Fax: + 613 9902 9500.

ORCID

Jacqueline A. Wilce: 0000-0002-8344-2626

Funding

This work was supported by a grant from the National Health and Medical Research Council awarded to J.A.W. (APP1045309)

Notes

The authors declare no competing financial interest.

ACKNOWLEDGMENTS

The authors thank all of the staff at the Monash Micro Imaging facility at Monash University for their assistance with the Leica AF6000 LX imaging system and Luxi Zhang for technical assistance.

ABBREVIATIONS

CPP, cell-penetrating peptide; DPI, dual-polarization interferometry; EGF, epidermal growth factor; FITC, fluorescein isothiocyanate; Grb7, growth factor receptor bound protein 7; NLS, nuclear localization signal; P7, truncated Penetratin; P16, full-length Penetratin; SH2, src homology 2; T_m, melting temperature; TNBC, triple-negative breast cancer

REFERENCES

(1) Ivanov, A. A.; Khuri, F. R.; Fu, H. Targeting protein-protein interactions as an anticancer strategy. *Trends Pharmacol. Sci.* **2013**, *34*, 393−400.

(2) Scott, D. E.; Bayly, A. R.; Abell, C.; Skidmore, J. Small molecules, big targets: drug discovery faces the protein-protein interaction challenge. *Nat. Rev. Drug Discovery* **2016**, *15*, 533−550.

(3) Bechara, C.; Sagan, S. Cell-penetrating peptides: 20 years later, where do we stand? *FEBS Lett.* **2013**, *587*, 1693−1702.

(4) Brock, R. The uptake of arginine-rich cell-penetrating peptides: putting the puzzle together. *Bioconjugate Chem.* **2014**, *25*, 863−868.

(5) Jain, M.; Chauhan, S. C.; Singh, A. P.; Venkatraman, G.; Colcher, D.; Batra, S. K. Penetratin improves tumor retention of single-chain antibodies: a novel step toward optimization of radioimmunotherapy of solid tumors. *Cancer Res.* **2005**, *65*, 7840−7846.

(6) Jo, D.; Liu, D.; Yao, S.; Collins, R. D.; Hawiger, J. Intracellular protein therapy with SOCS3 inhibits inflammation and apoptosis. *Nat. Med.* **2005**, *11*, 892−898.

(7) Perea, S. E.; Reyes, O.; Puchades, Y.; Mendoza, O.; Vispo, N. S.; Torrens, I.; Santos, A.; Silva, R.; Acevedo, B.; Lopez, E.; Falcon, V.; Alonso, D. F. Antitumor effect of a novel proapoptotic peptide that impairs the phosphorylation by the protein kinase 2 (casein kinase 2). *Cancer Res.* **2004**, *64*, 7127−7129.

(8) Plescia, J.; Salz, W.; Xia, F.; Pennati, M.; Zaffaroni, N.; Daidone, M. G.; Meli, M.; Dohi, T.; Fortugno, P.; Nefedova, Y.; Gabrilovich, D. I.; Colombo, G.; Altieri, D. C. Rational design of shepherdin, a novel anticancer agent. *Cancer Cell* **2005**, *7*, 457−468.

(9) Davidson, T. J.; Harel, S.; Arboleda, V. A.; Prunell, G. F.; Shelanski, M. L.; Greene, L. A.; Troy, C. M. Highly efficient small interfering RNA delivery to primary mammalian neurons induces MicroRNA-like effects before mRNA degradation. *J. Neurosci.* **2004**, *24*, 10040−10046.

(10) Muratovska, A.; Eccles, M. R. Conjugate for efficient delivery of short interfering RNA (siRNA) into mammalian cells. *FEBS Lett.* **2004**, *558*, 63−68.

(11) Frankel, A. D.; Pabo, C. O. Cellular uptake of the tat protein from human immunodeficiency virus. *Cell* **1988**, *55*, 1189−1193.

(12) Green, M.; Loewenstein, P. M. Autonomous functional domains of chemically synthesized human immunodeficiency virus tat trans-activator protein. *Cell* **1988**, *55*, 1179−1188.

(13) Joliot, A.; Pernelle, C.; Deagostini-Bazin, H.; Prochiantz, A. Antennapedia homeobox peptide regulates neural morphogenesis. *Proc. Natl. Acad. Sci. U.S.A.* **1991**, *88*, 1864−1868.

(14) Derossi, D.; Joliot, A. H.; Chassaing, G.; Prochiantz, A. The third helix of the Antennapedia homeodomain translocates through biological membranes. *J. Biol. Chem.* **1994**, *269*, 10444−10450.

(15) Fischer, P. M.; Zhelev, N. Z.; Wang, S.; Melville, J. E.; Fahraeus, R.; Lane, D. P. Structure-activity relationship of truncated and substituted analogues of the intracellular delivery vector Penetratin. *J. Pept. Res.* **2000**, *55*, 163−172.

(16) Stein, D.; Wu, J.; Fuqua, S. A.; Roonprapunt, C.; Yajnik, V.; D'Eustachio, P.; Moskow, J. J.; Buchberg, A. M.; Osborne, C. K.; Margolis, B. The SH2 domain protein GRB-7 is co-amplified,

DOI: 10.1021/acsomega.6b00561
ACS Omega 2017, 2, 670−677

overexpressed and in a tight complex with HER2 in breast cancer. *EMBO J.* **1994**, *13*, 1331−1340.
(17) Tanaka, S.; Pero, S. C.; Taguchi, K.; Shimada, M.; Mori, M.; Krag, D. N.; Arii, S. Specific peptide ligand for Grb7 signal transduction protein and pancreatic cancer metastasis. *J. Natl. Cancer Inst.* **2006**, *98*, 491−498.
(18) Wang, Y.; Chan, D. W.; Liu, V. W. S.; Chiu, P.; Ngan, H. Y. Differential functions of growth factor receptor-bound protein 7 (GRB7) and its variant GRB7v in ovarian carcinogenesis. *Clin. Cancer Res.* **2010**, *16*, 2529−2539.
(19) Tanaka, S.; Mori, M.; Akiyoshi, T.; Tanaka, Y.; Mafune, K.; Wands, J. R.; Sugimachi, K. Coexpression of Grb7 with epidermal growth factor receptor or Her2/erbB2 in human advanced esophageal carcinoma. *Cancer Res.* **1997**, *57*, 28−31.
(20) Akiyama, N.; Sasaki, H.; Ishizuka, T.; Kishi, T.; Sakamoto, H.; Onda, M.; Hirai, H.; Yazaki, Y.; Sugimura, T.; Terada, M. Isolation of a candidate gene, CAB1, for cholesterol transport to mitochondria from the c-ERBB-2 amplicon by a modified cDNA selection method. *Cancer Res.* **1997**, *57*, 3548−3553.
(21) Fiddes, R. J.; Campbell, D. H.; Janes, P. W.; Sivertsen, S. P.; Sasaki, H.; Wallasch, C.; Daly, R. J. Analysis of Grb7 recruitment by heregulin-activated erbB receptors reveals a novel target selectivity for erbB3. *J. Biol. Chem.* **1998**, *273*, 7717−7724.
(22) Pradip, D.; Bouzyk, M.; Dey, N.; Leyland-Jones, B. Dissecting GRB7-mediated signals for proliferation and migration in HER2 overexpressing breast tumor cells: GTP-ase rules. *Am. J. Cancer Res.* **2013**, *3*, 173−195.
(23) Chu, P.-Y.; Li, T.-K.; Ding, S.-T.; Lai, I.-R.; Shen, T.-L. EGF-induced Grb7 recruits and promotes Ras activity essential for the tumorigenicity of Sk-Br3 breast cancer cells. *J. Biol. Chem.* **2010**, *285*, 29279−29285.
(24) Bai, T.; Luoh, S.-W. GRB-7 facilitates HER-2/Neu-mediated signal transduction and tumor formation. *Carcinogenesis* **2007**, *29*, 473−479.
(25) Pero, S. C.; Oligno, L.; Daly, R. J.; Soden, A. L.; Liu, C.; Roller, P. P.; Li, P.; Krag, D. N. Identification of novel non-phosphorylated ligands, which bind selectively to the SH2 domain of Grb7. *J. Biol. Chem.* **2002**, *277*, 11918−11926.
(26) Giricz, O.; Calvo, V.; Pero, S. C.; Krag, D. N.; Sparano, J. A.; Kenny, P. A. GRB7 is required for triple-negative breast cancer cell invasion and survival. *Breast Cancer Res. Treat.* **2012**, *133*, 607−615.
(27) Pero, S. C.; Shukla, G. S.; Cookson, M. M.; Flemer, S., Jr.; Krag, D. N. Combination treatment with Grb7 peptide and Doxorubicin or Trastuzumab (Herceptin) results in cooperative cell growth inhibition in breast cancer cells. *Br. J. Cancer* **2007**, *96*, 1520−1525.
(28) Ambaye, N. D.; Lim, R. C.; Clayton, D. J.; Gunzburg, M. J.; Price, J. T.; Pero, S. C.; Krag, D. N.; Wilce, M. C. J.; Aguilar, M.-I.; Perlmutter, P.; Wilce, J. A. Uptake of a cell permeable G7-18NATE construct into cells and binding with the Grb-7-SH2 domain. *Biopolymers* **2011**, *96*, 181−188.
(29) Shamay, Y.; Adar, L.; Ashkenasy, G.; David, A. Light induced drug delivery into cancer cells. *Biomaterials* **2011**, *32*, 1377−1386.
(30) Lin, W.; Xie, X.; Deng, J.; Liu, H.; Chen, Y.; Fu, X.; Liu, H.; Yang, Y. Cell-penetrating peptide-doxorubicin conjugate loaded NGR-modified nanobubbles for ultrasound triggered drug delivery. *J. Drug Targeting* **2015**, *24*, 134−146.
(31) Bahnsen, J. S.; Franzyk, H.; Sandberg-Schaal, A.; Nielsen, H. M. Antimicrobial and cell-penetrating properties of penetratin analogs: effect of sequence and secondary structure. *Biochim. Biophys. Acta* **2013**, *1828*, 223−232.
(32) Khafagy, E.-S.; Morishita, M.; Ida, N.; Nishio, R.; Isowa, K.; Takayama, K. Structural requirements of penetratin absorption enhancement efficiency for insulin delivery. *J. Controlled Release* **2010**, *143*, 302−310.
(33) Fischer, R.; Waizenegger, T.; Kohler, K.; Brock, R. A quantitative validation of fluorophore-labelled cell-permeable peptide conjugates: fluorophore and cargo dependence of import. *Biochim. Biophys. Acta* **2002**, *1564*, 365−374.
(34) Richard, J. P.; Melikov, K.; Vives, E.; Ramos, C.; Verbeure, B.; Gait, M. J.; Chernomordik, L. V.; Lebleu, B. Cell-penetrating peptides. A reevaluation of the mechanism of cellular uptake. *J. Biol. Chem.* **2003**, *278*, 585−590.
(35) Hirst, D. J.; Lee, T.-H.; Kulkarni, K.; Wilce, J. A.; Aguilar, M.-I. The impact of cell-penetrating peptides on membrane bilayer structure during binding and insertion. *Biochim. Biophys. Acta* **2016**, *1858*, 1841−1849.
(36) Pace, C. N.; Vajdos, F.; Fee, L.; Grimsley, G.; Gray, T. How to measure and predict the molar absorption coefficient of a protein. *Protein Sci.* **1995**, *4*, 2411−2423.
(37) van Dalen, J. P. R.; Haaijman, J. J. Determination of the molar absorbance coefficient of bound tetramethyl rhodamine isothiocyanate relative to fluorescein isothiocyanate. *J. Immunol. Methods* **1974**, *5*, 103−106.
(38) Porter, C. J.; Wilce, J. A. NMR analysis of G7-18NATE, a nonphosphorylated cyclic peptide inhibitor of the Grb7 adapter protein. *Biopolymers* **2007**, *88*, 174−181.
(39) Watson, G. M.; Gunzburg, M. J.; Ambaye, N. D.; Lucas, W. A. H.; Traore, D. A.; Kulkarni, K.; Cergol, K. M.; Payne, R. J.; Panjikar, S.; Pero, S. C.; Perlmutter, P.; Wilce, M. C. J.; Wilce, J. A. Cyclic peptides incorporating phosphotyrosine mimetics as potent and specific inhibitors of the Grb7 breast cancer target. *J. Med. Chem.* **2015**, *58*, 7707−7718.

DOI: 10.1021/acsomega.6b00561
ACS Omega 2017, 2, 670−677